Molecular Pharmacology Fast Forward. Published on March 20, 2017 as DOI: 10.1124/mol.116.107409
This article has not been copyedited and formatted. The final version may differ from this version.

Thiosemicarbazones Functioning as Zinc Metallochaperones to Reactivate Mutant p53

Xin Yu, Adam Blanden, Ashley T. Tsang, Saif Zaman, Yue Liu, John Gilleran, Anthony F. Bencivenga, S. David Kimball, Stewart N. Loh, and Darren R. Carpizo

Rutgers Cancer Institute of New Jersey (XY, ATT, SZ, YL, DRC), Department of Surgery, Rutgers Robert Wood Johnson Medical School (XY, ATT, YL, DRC), Rutgers Translational Sciences, Department of Chemistry and Chemical Biology (SDK), Department of Medicinal Chemistry, Rutgers Ernest Mario School of Pharmacy (JG, AFB, SDK), Rutgers University, New Brunswick, NJ, USA, Department of Biochemistry and Molecular Biology, SUNY Upstate Medical University, Syracuse, NY, USA (AB, SNL), Mount Sinai St. Luke's Roosevelt General Surgery Residency Program, New York, NY, USA (ATT).

Molecular Pharmacology Fast Forward. Published on March 20, 2017 as DOI: 10.1124/mol.116.107409
This article has not been copyedited and formatted. The final version may differ from this version.

RUNNING TITLE

Running Title: Thiosemicarbazones reactivate mutant p53 as Zn Metallochaperones

Corresponding author: Darren R. Carpizo

Address: Rutgers Cancer Institute of New Jersey, 195 Little Albany Street, New Brunswick, NJ 08903, USA

Telphone: 732-235-8524

Fax: 732-235-8098

Email address: carpizdr@cinj.rutgers.edu

Corresponding author: Stewart N Loh

Address: Department of Biochemistry and Molecular Biology, SUNY-Upstate Medical University, 4249 Weiskotten Hall, 766 Irving Avenue, Syracuse, NY 13210, USA

Telphone: 315-464-8731

Email address: lohs@update.edu

Number of text pages: 34

Number of Figures: 5

Number of Tables: 1

Number of references: 31

Number of words in Abstract: 244

Number of words in Introduction: 712

Number of words in Discussion: 786

Molecular Pharmacology Fast Forward. Published on March 20, 2017 as DOI: 10.1124/mol.116.107409
This article has not been copyedited and formatted. The final version may differ from this version.

Nonstandard Abbreviations (listed alphabetically):

3-AP—Triapine

CF—carboxyfluorescein

DBD—DNA binding domain

DOPC—1,2-dioleoyl-sn-glycero-3-phosphocholine

PAR—4-(2-Pyridylazo)resorcinol

ROS—reactive oxygen species

RZ-3—RhodZin-3

TCEP—tris(2-carboxyethyl)phosphine hydrochloride

TSC—thiosemicarbazone

WT—wild type

ZMCs—zinc metallochaperones

Molecular Pharmacology Fast Forward. Published on March 20, 2017 as DOI: 10.1124/mol.116.107409
This article has not been copyedited and formatted. The final version may differ from this version.

ABSTRACT

Small molecule restoration of wild type structure and function to mutant p53 (so–called mutant reactivation) is a highly sought after goal in cancer drug development. We previously discovered small molecule zinc chelators called zinc metallochaperones (ZMCs) reactivate mutant p53 by restoring zinc binding to zinc deficient p53 mutants. The lead compound identified from the NCI-60 human tumor cell lines screen, NSC319726 (ZMC1), belongs to the thiosemicarbazone (TSC) class of metal ion chelators that bind Fe, Cu, Mn, Zn, and other transition metals. Here, we investigate the other TSCs, NSC319725, NSC328784 identified in the same screen, as well as the more well studied TSC, 3-AP (Triapine), to determine if they function as ZMCs. We measured the zinc K_d, zinc ionophore activity, ability to restore zinc to purified p53 DNA binding domain (DBD), and ability to restore site-specific DNA binding to purified R175H-DBD in vitro. We tested all four TSCs in a number of cell based assays to examine mutant p53 reactivation and the generation of reactive oxygen species (ROS). We found that NSC319725 and NSC328784 behave similarly to ZMC1 in both biophysical and cell-based assays, and are heretofore named ZMC2 (NSC319725) and ZMC3 (NSC328784). 3-AP generates a ROS signal similar to ZMC1-3, but fails to function as a ZMC both in vitro and in cells and ultimately does not reactivate p53. These findings indicate that not all TSCs function as ZMCs, and much of their activity can be predicted by their affinity for zinc.

Molecular Pharmacology Fast Forward. Published on March 20, 2017 as DOI: 10.1124/mol.116.107409
This article has not been copyedited and formatted. The final version may differ from this version.

INTRODUCTION

TP53 is the most commonly mutated gene in human cancer and plays an essential role as a tumor suppressor (Bieging et al., 2014; Freed-Pastor and Prives, 2012; Levine and Oren, 2009). The majority of mutations (>70%) are missense and generate a defective protein generally found at high levels in cancer cells due to loss of MDM2-mediated negative feedback (Haupt et al., 1997). Restoring wild type (WT) p53 function by genetic means in mouse models of cancer triggers potent anti-cancer activity (Ventura et al., 2007; Xue et al., 2007). Thus, reactivation of WT structure/function of mutant p53 using small molecules has been an area of intense investigation in anti-cancer drug development.

The p53 protein requires the binding of a single zinc ion for proper folding. There is now evidence that manipulating zinc concentrations can change the structure/function of WT p53, indicating that the structure is malleable (Butler and Loh, 2003; Hainaut and Milner, 1993; Meplan et al., 2000). This concept also applies to certain mutant p53s in which the mutated amino acid impairs the protein's ability to coordinate zinc and causes misfolding. There are three major classes of mutant p53 proteins: destabilizing, DNA-contact, and zinc-binding, each of which impairs the protein for different reasons and presents its own unique challenges for targeted drug development. The zinc-binding class is best exemplified by the most common p53 mutant found in cancer, p53-R175H.

Using an *in silico* screen of the NCI-60 human tumor cell lines screen anti-cancer drug database, we previously identified three small molecules (NSC319725, NSC319726, NSC328784) that belong to the thiosemicarbazone (TSC) family of metal ion chelators with high activity in cell lines with mutant p53 (Yu et al., 2012a). We went on to

Molecular Pharmacology Fast Forward. Published on March 20, 2017 as DOI: 10.1124/mol.116.107409
This article has not been copyedited and formatted. The final version may differ from this version.

demonstrate that NSC319726 (ZMC1) kills cancer cells by restoring the wild type structure and function of p53-R175H both *in vitro* and *in vivo* (Yu et al., 2012a). We elucidated the ZMC1 mechanism by finding that: 1) ZMC1 is a zinc metallochaperone (ZMC) that delivers zinc to p53-R175H by functioning as a zinc ionophore, thus allowing the mutant to fold properly; and 2) ZMC1 boosts intracellular reactive oxygen species (ROS), which transactivates the newly conformed mutant through amino-terminal post-translational modifications (Blanden et al., 2015b; Yu et al., 2014). Importantly, we found that other zinc chelators with a similar affinity (K_d) for zinc can function as ZMCs to restore wild type conformation to p53-R175H (Butler and Loh, 2003; Hainaut and Milner, 1993).

The model for ZMC restoration of WT p53 structure posits two types of zinc ligation sites on p53: native (K_{d1}) and non-native (K_{d2}) (Yu et al., 2014). We experimentally determined the K_{d1} of the R175H DBD to be on the order of 10^{-9} M, which is 10-1000-fold higher than physiological zinc concentrations (10^{-12}-10^{-10} M), indicating that R175H is likely in the apo (zinc-free) form in the cell (Bozym et al., 2006). Raising intracellular zinc above 10^{-9} M can in principle restore WT conformation to R175H, but if levels rise above the dissociation constant of the non-native ligation sites (K_{d2} ~10^{-6}) the protein will again misfold. ZMCs like ZMC1 restore wild type structure to mutant p53 by raising intracellular zinc concentrations to greater than the K_{d1} of the p53-R175H while at the same time functioning as zinc buffers to prevent zinc induced misfolding.

Thiosemicarbazones have an affinity for divalent metal ions such as Fe^{2+}, Zn^{2+}, Cu^{2+}, and Mn^{2+}, and been investigated as anti-cancer drugs, the most notable being 3-

Molecular Pharmacology Fast Forward. Published on March 20, 2017 as DOI: 10.1124/mol.116.107409
This article has not been copyedited and formatted. The final version may differ from this version.

aminopyridine-2-carboxaldehyde (3-AP or Triapine®) (Finch et al., 2000). 3-AP is currently in phase II clinical trials for aggressive myeloproliferative neoplasms, advanced-stage cervical and vaginal cancers, advanced renal carcinoma, advanced non-small cell lung cancer (Kunos et al., 2013; Yu et al., 2012b; Zeidner et al., 2014). The mechanism of action of TSCs has been attributed to the inhibition of the iron-dependent enzyme ribonucleotide reductase as well as TSC-Fe complexes that contribute to cell death by facilitating Fenton chemistry and increasing oxidative stress (Richardson et al., 2006; Shao et al., 2006). These features have plagued the development of these drugs due to toxicities related to methemoglobinemia and bone marrow suppression among others (Ma et al., 2008; Murren et al., 2003). Given that NSC319725 and NSC328784 as well as 3-AP all belong to the same chemical class, we sought to investigate if these compounds could function as zinc metallochaperones to reactive mutant p53 in addition to any other reported activities.

MATERIALS AND METHODS

Chemicals

NSC319726 (ZMC1), NSC319725 (hereafter, ZMC2) and NSC328784 (hereafter ZMC3) were synthesized by the Rutgers Translational Sciences group. 3-AP was purchased from Sigma-Aldrich. 1,2-dioleoyl-sn-glycero-3-phosphocholine (DOPC) was purchased from Avanti Polar Lipids (Alabaster, AL). RhodZin-3 (RZ-3) was purchased from Life Technologies Corporation (Norwalk, CT). MTS reagent was purchased from Promega. All other chemicals were purchased from Sigma-Aldrich or otherwise indicated.

Molecular Pharmacology Fast Forward. Published on March 20, 2017 as DOI: 10.1124/mol.116.107409
This article has not been copyedited and formatted. The final version may differ from this version.

Protein preparation

The p53 (94-312) DNA Binding Domains (DBD) were expressed and purified as described previously (Yu et al., 2014). Apo proteins were generated as described previously (Butler and Loh, 2003). All experiments were performed in 50 mM Tris (pH 7.2), 0.1 M NaCl, and 1 mM tris(2-carboxyethyl)phosphine hydrochloride (TCEP) unless otherwise noted.

Spectroscopic measurements

Absorbance experiments were performed in a Varian Cary-100 UV-Visible spectrophotometer equipped with thermostatted cuvette holder. Fluorescence experiments were performed on a Fluoromax-4 spectrofluorimeter equipped with thermostatted cuvette holder (Jobin-Yvon). Fluorescence measurements were recorded in a 1 cm by 1 cm quartz cuvette with excitation and emission slits of 3 nm and 4 nm respectively. All experiments were conducted at 10 ˚C unless otherwise noted.

RZ-3-Zn^{2+} competition assay

RZ-3 at 100 nM and $ZnCl_2$ at 50 nM were incubated with the indicated concentration of TSC in buffer with 4% v/v DMSO at room temperature and allowed to equilibrate for >1 h. RZ-3 fluorescence was then measured and the IC50 determined by fitting to a sigmoid curve on a semi-log axis. This IC_{50} value was then divided by 2 to account for the known 2:1 binding stoichiometry of these compounds, and apparent K_d calculated according to the Munson-Robard exact solution to the Cheng-Prussof equation:

Molecular Pharmacology Fast Forward. Published on March 20, 2017 as DOI: 10.1124/mol.116.107409
This article has not been copyedited and formatted. The final version may differ from this version.

$$K_i = \frac{IC50}{1 + \frac{L_T(y_0 + 2)}{2K_d(y_0 + 1)} + y_0} - K_d \frac{y_0}{y_0 + 2}$$

Eqn 1

where K_i = the apparent K_d of the TSC, L_T is the total concentration of RZ-3 (100 nM), K_d is the dissociation constant of RZ-3 for Zn^{2+} (65 nM per manufacturer), and y_0 is the ratio of bound RZ-3 to free RZ-3 in the absence of TSC (26.5 nM/73.5 nM under these conditions).

Arrested refolding

Arrested refolding experiments were performed as described previously with minor modifications (Butler and Loh, 2007). DBD (25 μM) was denatured in buffer containing 5 M urea, and then rapidly diluted 50-fold into urea-free buffer with or without 2.5 μM $ZnCl_2$ to final concentrations 0.5 μM DBD and 0.1 M urea with continuous magnetic stirring. Intrinsic tryptophan fluorescence was monitored at the absorbance isosbestic point between the Zn^{2+}-bound and Zn^{2+}-free forms of the drug to minimize changes in inner-filter effect throughout the experiment (ZMC2 338 nm, ZMC3 355 nm, 3-AP 376 nm, excitation 280 nm). For $ZnCl_2$-containing samples, after ~90 s of stalled-folding, the indicated concentration of EDTA, compounds, or DMSO vehicle was added and folding monitored as before. Kinetic traces were corrected for inner-filter effect empirically.

Zn^{2+} content measurement

DBD samples were desalted using a PD-10 column (Amersham) equilibrated 50 mM Tris (pH 7.2), 150 mM NaCl, and 1 mM TCEP. Samples (1-10 μM) were then unfolded in 6 M Gdn-HCl and reacted with 1 mM N-ethylmaleimide for 20 m at RT to ensure complete

Molecular Pharmacology Fast Forward. Published on March 20, 2017 as DOI: 10.1124/mol.116.107409
This article has not been copyedited and formatted. The final version may differ from this version.

release of all bound Zn^{2+}. The reaction was quenched with 10 mM β-ME for 10 m, and Zn^{2+} concentration measured by adding 150 μM 4-(2-Pyridylazo)resorcinol (PAR) and measuring the absorbance blanked against PAR in buffer using $\epsilon_{500} = 5.0 \times 10^4\ M^{-1}\ cm^{-1}$ for the PAR_2Zn complex in buffer containing 6 M Gdn-HCl as determined by our lab. Measured Zn^{2+} concentration was divided by protein concentration to determine Zn^{2+} content of the protein.

Re-metallation

After apoization, DBD (15-30 μM) was incubated with a mixture of 60 μM $ZnCl_2$, 180 μM compound for 20 min on ice. Samples were then desalted and Zn^{2+} content assayed as above. For Zn2+-remetallation experiments, data for WT and R175H DBD were analyzed separately via one-way ANOVA, and then all pairwise comparisons were analyzed with the Holm-Sidak method for multiple comparisons with an overall significance level of $p<0.05$ in SigmaPlot 13.0.

Ionophore Assay

DOPC-liposomes (100 nm) were prepared by film rehydration and extrusion as described previously (Blanden et al., 2015b). RZ-3 and carboxyfluorescein (CF) were encapsulated at 10 μM and 100 mM respectively. Liposome solutions were diluted to $OD_{600} < 0.02$ before use, and measurements taken in a 5 mm x 5 mm quartz cuvette at room temperature. Excitation and emission wavelengths were 550/572 nm for RZ-3 and 492/512 nm for CF.

Molecular Pharmacology Fast Forward. Published on March 20, 2017 as DOI: 10.1124/mol.116.107409
This article has not been copyedited and formatted. The final version may differ from this version.

Cell lines and culture conditions

TOV112D and H1299 were cultured in DMEM with 10% FBS. H460, SKBR3, and HOP92 were cultured in RPMI with 10% FBS.

Cell growth inhibition assay

MTS assay was performed according to the manufacturer's instructions (Promega). In brief, 5000 cells per well were cultured in 96-well plate to reach the 50% confluence on the second day when treated with serial dilutions of the compounds. Growth was measured by MTS reagent and Victor Plate reader instrument (PerkinElmer) after incubation for 3 d.

Transfection of p53 siRNA

The siRNA transfection is done with Lipofectamine RNAiMAX (Invitrogen), following the manufacture's instuctions. The p53 siRNA was from SMARTpool (Thermo Fisher Scientific/Dharmacon). The cells after 24-hour transfection were reseeded to 96-well plate for treatment of the compounds and the cell growth inhibition was measured by CellTiter-Glo (Promega) according to the manufacture's instruction. Statistical significance of the data, obtained from two independent experiments, each with triplicates, was calculated with Student's *t*-test.

Colony formation assays

For long-term viability, one thousand cells per well on 6-well plate were treated with the compounds with various concentrations for 6 hours, then, cells were cultured with drug-

Molecular Pharmacology Fast Forward. Published on March 20, 2017 as DOI: 10.1124/mol.116.107409
This article has not been copyedited and formatted. The final version may differ from this version.

free complete medium for 10 days with fresh medium without interference. Cells were fixed with 10% formalin and stained with 0.05% crystal violet at the end of 10-day period of cell culture (Franken et al., 2006). Statistical significance of the data, obtained from three independent experiments, each with triplicates, was calculated with Student's *t*-test.

Immunofluorescent staining

Cells were grown on coverslips, followed by various treatments. The coverslips were fixed with 4% paraformaldehyde for 10 min and then permeabilized with 0.5% Triton-X100 for 5 min. The conformation of the mutant and WT p53 proteins were recognized specifically by the antibodies PAB1620 (1:50, recognizing WT conformation) and PAB240 (1:400, recognizing misfolded/unfolded conformation) stained overnight, respectively. The secondary antibody, goat anti-mouse IgG was incubated for 40 m. PAB1620 and PAB240 were purchased from EMD Chemicals.

RNA extraction and quantitative RT-PCR

RNA was extracted from the cells using RNeasy kit (Qiagen) and the gene expression level was measured by quantitative RT-PCR using TaqMan gene expression assays (Life Technologies/Applied BioSystems). The gene expression level was normalized with β-actin and the average was presented with standard deviation. Statistical significance of the data was calculated by Student's *t*-test.

Western blot

Molecular Pharmacology Fast Forward. Published on March 20, 2017 as DOI: 10.1124/mol.116.107409
This article has not been copyedited and formatted. The final version may differ from this version.

The cell lysates were run on SDS-PAGE and transferred onto PVDF membranes. The detection of the protein level was performed with the manufacturer's instructions (Western Lightning® Plus-ECL, Perkin-Elmer). The p21 antibody was purchased from EMD Chemicals. The actin antibody was purchased from Santa Cruz Biotechnology.

8-oxy-dG staining

8-oxy-dG (Clone 2E2) antibody was purchased from Trevigen. Immunocytochemistry staining followed the manufacturer's instructions. The staining was quantified by density/brightness using ImageJ. Statistical significance of the data was calculated by Student's *t*-test.

Electrophoretic mobility shift assay (EMSA)

Purified p53 apoDBD (R175H) was used in the indicated reactions. DNA was 44-bp p53 recognition sequence (p53RE) in the promoter sequence of p21 gene (Lokshin et al., 2007), 5' F-AGCTAGTAGAGCGAACATGTCCCAACATGTTGGCGTGCTGCAGC, 5' R-GCTGCAGCACGCCAACATGTTGGGACATGTTCGCTCTACTAGCT. DNA was labeled with biotin with a DNA 3' end biotinylation kit (Thermo Fisher Scientific/Pierce). The reaction mixture was incubated at 4°C for 10 m prior to addition of biotin-labeled probes. Binding buffer was described previously (Lokshin et al., 2007). DNA binding reactions were carried out at 4 °C for 20 min, and the resulting DNA-protein complexes were separated on a 6% polyacrylamide gel (made with 30% Acrylamide/Bis Solution (37.5:1) (Bio-Rad)) in 0.5× Tris-borate (without EDTA), running in 0.5× Tris-borate

Molecular Pharmacology Fast Forward. Published on March 20, 2017 as DOI: 10.1124/mol.116.107409
This article has not been copyedited and formatted. The final version may differ from this version.

(without EDTA) buffer. Complexes were visualized by LightShift Chemiluminescent EMSA Kit (Thermo Fisher Scientific/Pierce).

Statistical Methods

For Zn2+-remetallation experiments, data for WT and R175H DBD were analyzed separately via one-way ANOVA, and then all pairwise comparisons were analyzed with the Holm-Sidak method for multiple comparisons with an overall significance level of $p<0.05$ in SigmaPlot 13.0. The other data were analyzed by Student's *t*-test with an overall significance level of $p<0.05$. *$p<0.05$, **$p<0.01$, ***$p<0.001$.

RESULTS

ZMC2 and ZMC3 exhibit zinc metallochaperone properties, while 3-AP does not.

ZMC1, ZMC2, ZMC3 and 3-AP are heteroaromatic substituted TSCs and share the characteristic N-N-S(Se) backbone of a general thio- and selenosemicarbazone. The chemical structures are depicted in Figure 1A.

To both chelate zinc in the extracellular space and donate zinc to mutant p53, ZMCs must bind zinc with an affinity similar to that of the native site on DBD. We previously determined the zinc K_d of ZMC1 to be ~30 nM (Yu et al., 2014). To determine if ZMC2, ZMC3, and 3-AP bind Zn^{2+} in the affinity range of a ZMC, which according to our current understanding of the ZMC mechanism is ~10^{-9}-10^{-6} M (Blanden et al., 2015a; Blanden et al., 2015b; Yu et al., 2014). we measured their apparent Zn^{2+} K_d by competition with fluorescent Zn^{2+}-chelator RZ-3 (Fig. 1B). ZMC2 and ZMC3 both bound with a K_d in the range required for R175H reactivation (27.4 ± 16.2 nM and 81 ±

Molecular Pharmacology Fast Forward. Published on March 20, 2017 as DOI: 10.1124/mol.116.107409
This article has not been copyedited and formatted. The final version may differ from this version.

34.2 nM, respectively). 3-AP did not bind Zn^{2+} under the assay conditions, which corresponds to $K_d > 1$ μM and is above the upper limit required by the ZMC model.

To evaluate the ability of ZMC2, ZMC3, and 3-AP to remetallate apoDBD, as is required for Zn^{2+}-deficient p53 reactivation, we incubated WT and R175H apoDBD with a 3:1 mixture of TSC:$ZnCl_2$ and assayed the resultant Zn^{2+} content of the proteins using colorimetric Zn^{2+} indicator PAR (Fig. 1C). All three compounds were able to restore the Zn^{2+}-content of the apo proteins, with ZMC3 and 3-AP restoring more Zn^{2+} than ZMC2. However, when we assayed the foldedness of the remetallated proteins by intrinsic tryptophan fluorescence, leveraging the known property of DBD to increase in fluorescence when it misfolds (Yu et al., 2014), we found that the proteins remetallated with ZMC2 and ZMC3 were native and the proteins remetallated with 3-AP were misfolded (Fig. 1D).

We then evaluated the ability of ZMC2, ZMC3, and 3-AP to rescue the folding of DBDs that had previously been misfolded by excess Zn^{2+}, a known property of synthetic ZMCs (Fig. 1E-G, Supplemental Fig. 1) (Butler and Loh, 2007; Yu et al., 2014). Briefly, WT and R175H DBD were unfolded in urea and then refolded by rapid dilution in the presence or absence of excess $ZnCl_2$. In the presence of excess $ZnCl_2$, the proteins become trapped in the highly fluorescent misfolded state. After ~60s, a 4-fold molar excess of TSC (2 binding equivalents) was added and refolding monitored by fluorescence as DBD converted from the highly fluorescent misfolded state to the weakly fluorescent native state. Both ZMC2 and ZMC3 efficiently rescued the folding of R175H and WT DBD with equal or superior efficiency relative to the known Zn^{2+}-chelator EDTA, whereas 3-AP had no effect on either.

Molecular Pharmacology Fast Forward. Published on March 20, 2017 as DOI: 10.1124/mol.116.107409
This article has not been copyedited and formatted. The final version may differ from this version.

To confirm that the conformation induced by ZMC2 and ZMC3 was WT, we turned to the electrophoretic mobility shift assays (EMSA) to evaluate whether the TSCs and zinc could restore site-specific binding to apo R175H DBD using a DNA oligonucleotide bearing the p21 recognition sequence (Fig. 1H). Previously, we demonstrated that ZMC1 only in the presence of zinc could restore site-specific DNA binding to the R175H DBD (Yu et al., 2014). Using the EMSA, we evaluated ZMC2, ZMC3 and 3-AP using ZMC1 as a positive control and A6 as a negative control. A6 is an analog of ZMC1 whose ZMC activity has been abolished by ~30-fold decrease in zinc binding (Yu et al., 2014). The combination of 10 μM $ZnCl_2$ and 20 μM ZMC1 (Lane 3), ZMC2 (Lane 4) and ZMC3 (lane 5) restored DNA binding to R175H apoDBD, but not with 3-AP (Lane 6), A6 (Lane 7), or apoDBD alone (Lane 2).

We then evaluated the compounds for ionophore activity as required by the ZMC mechanism. Briefly, we encapsulated fluorescent Zn^{2+}-indicator RZ-3 in DOPC-liposomes and monitored Zn^{2+} transport into the liposomes using the increase RZ-3 fluorescence upon Zn^{2+} binding as previously described (Blanden et al., 2015b). Both ZMC2 and ZMC3 caused a significant increase in the rate of Zn^{2+} transport into the liposomes. 3-AP caused no detectible increase. The increase in RZ-3 fluorescence was completely reversible upon detergent lysis and addition of excess EDTA, indicating that the increase was caused exclusively by metal binding. We also performed a non-specific leakage control using self-quenching fluorophore carboxyfluorescein (CF), and found no non-specific leakage from the liposomes for any of the compounds (Fig. 1I-K) (Blanden et al., 2015b). Taken together, these data indicate that ZMC2 and ZMC3 fulfill both the

Molecular Pharmacology Fast Forward. Published on March 20, 2017 as DOI: 10.1124/mol.116.107409
This article has not been copyedited and formatted. The final version may differ from this version.

Zn^{2+}-buffering and ionophore requirements for a p53 reactivating ZMC *in vitro*, but 3-AP does not.

ZMC2 and ZMC3, but not 3-AP, demonstrate enhanced sensitivity in p53-R175H mutant cells.

One of the cellular properties of a ZMC is enhanced sensitivity in p53-R175H cells lines that is a log fold or greater than that of p53 null or WT cell lines in cell growth inhibition assays (manifested by lower EC_{50}'s) (Yu et al., 2014; Yu et al., 2012a). This enhanced sensitivity is due to a p53 mediated apoptotic program. We sought to evaluate ZMC2, ZMC3 and 3-AP for this property using ZMC1 as a control in human tumor cell lines that were WT, null and p53-R175 mutant (Fig. 2). All three ZMC compounds exhibited growth inhibition at markedly lower concentrations in cells expressing mutant $p53^{R175H}$ as compared to the WT or p53-null controls (Fig. 2A). The EC_{50}s for ZMC2 and ZMC1 were similar in treated p53-R175H mutant cells (EC_{50} 0.87 μM). The EC_{50} of ZMC3 was approximately 6-fold higher (EC_{50} 3.40 μM) but was still preferentially toxic for the p53-R175H cell lines as the EC_{50} in the WT and null cell lines was not reached. In contrast, 3-AP does not exhibit increased sensitivity in p53-R175H cells as compared to p53-WT or p53-null cells (Table 1). To verify that the observed growth inhibition is p53-dependent, we used siRNA to *TP53* to knockdown the expression of p53 and measured the cell growth in response to drug treatment. ZMC2 and ZMC3, like ZMC1, showed differential cellular sensitivity but 3-AP did not (Fig. 2B). Finally to more closely approximate mimic the conditions in a treated tumor, we sought to evaluate the effects of a 6 hour drug treatment over a longer duration of time (as compared to the 3 day drug

Molecular Pharmacology Fast Forward. Published on March 20, 2017 as DOI: 10.1124/mol.116.107409
This article has not been copyedited and formatted. The final version may differ from this version.

exposure) using the colony formation assay. After 10 days, ZMC2 and ZMC3, like ZMC1, showed no growth in 0.1 and 1 μM treatment, while 3-AP showed a greater number of colonies than the untreated control (Fig. 2C-D).

Induction of a "WT-like" conformational change in the p53^{R175} mutant cells by TSCs.

Another cellular hallmark of a ZMC is the ability to induce a conformation change from mutant to wild type in the p53-R175H protein (Yu et al., 2014; Yu et al., 2012a). Using conformation specific antibodies and immunofluorescent staining the p53^{R175H} cells (TOV112D and SKBR3), we observed that ZMC2 and ZMC3, like ZMC1, induced a conformation change in the p53^{R175H} mutant to a structure that was recognized by the WT specific antibody (PAB1620) and was no longer recognized by the mutant specific antibody (PAB240) (Fig. 3). In contrast, 3-AP failed to induce such a change.

Restoration of wild type p53 transcriptional function by the TSCs.

To determine if the conformation change observed with the p53^{R175} mutant resulted in restoration of WT p53 transcriptional function, we compared the mRNA levels of two p53 targets (*p21*, *PUMA*) in the p53^{R175H} cells (TOV112D and SKBR3). We found that, similar to ZMC1, ZMC2 and ZMC3 increased the levels of the p53 target genes in these cells, but no such increase was seen for 3-AP (Fig. 4A).

We then examined p21 protein levels at 6 and 24 hours after treatment in TOV112D and SKBR3 cells and found that ZMC2 and ZMC3 induced p21 robustly in both cell lines (Fig. 4B). 3-AP demonstrated a weak induction of p21 in the TOV112D cells and no induction in the SKBR3 cell line. The time course of the p21 induction by 3-

Molecular Pharmacology Fast Forward. Published on March 20, 2017 as DOI: 10.1124/mol.116.107409
This article has not been copyedited and formatted. The final version may differ from this version.

AP was also different. ZMCs typically induce p21 maximally by ~6 h, followed by a fall-off approaching basal levels by 24 h. This suggests that the p21 induction in TOV112D cells by 3-AP was more likely p53 independent.

TSCs induce cellular ROS levels.

One of the features of TSCs is that they induce cellular ROS levels. We previously demonstrated that the ZMC1 ROS induction plays an important role in the ZMC mechanism by serving as a cellular stress response that transcriptionally activates the refolded WT-like mutant protein through post-translational modifications, including phosphorylation events on serines 15 and 46 and acetylation events on lysine 120, all of which function to direct mutant p53 to induce an apoptotic program (Yu et al., 2014). To confirm that these three TSCs induce ROS in cells, we performed immunofluorescent staining on the treated cells using an antibody that detects oxidized DNA (8-oxy-dGuo) on human tumor cell lines of different p53 status. We found that all of the tested compounds increased the 8-oxy-dGuo staining in both the TOV112D ($p53^{R175H}$) and the H1299 ($p53^{-/-}$) cells at 24 hours (Fig. 5A). Quantitatively, all four TSCs induce ROS levels from 2-4 fold above baseline in TOV112D cells (Fig. 5B).

DISCUSSION

The thiosemicarbazone class of metal ion chelators has been reported to demonstrate a broad spectrum of pharmacologic activity including antineoplastic, antiviral, antifungal, and antimalarial, all of which is due to their antiproliferative activity (Beraldo and Gambino, 2004). Their ability to chelate metal ions such as Fe, Cu, and Zn depends on

Molecular Pharmacology Fast Forward. Published on March 20, 2017 as DOI: 10.1124/mol.116.107409
This article has not been copyedited and formatted. The final version may differ from this version.

an N-N-S backbone structure that functions in metal ion binding (Yu et al., 2009). This is exemplified by the α-pyridyl thiosemicarbazones in which the N_{pyr}, N^1, and S participate in metal ligand binding. All four compounds in this study are either α-pyridyl TSCs, or a closely related selenosemicarbazone in the case of ZMC3, in which the chalcogen donor atom is selenium. Coordination chemistry of α-pyridyl thiosemicarbazones is typically 2 molecules of TSC to one molecule of metal ion combined with a proton ionization from each TSC molecule, forming a charge neutral 2:1 coordination complex with octahedral geometry. We hypothesize that the charge neutrality contributes to the observed ability of TSC-metal ion complexes to passively diffuse through cell membranes. We previously validated this concept for ZMC1 using X-ray crystallography to demonstrate that the ZMC1-Zn forms a neutral, 2:1 octahedral complex, and that it functions as a zinc ionophore to raise intracellular zinc concentrations (Blanden et al., 2015b).

The mechanism of action of TSCs as anticancer drugs has been mostly attributed to their chelation of Fe. TSC-Fe complexes are redox active and thus generate hydroxyl radicals through the oxidation of H_2O_2 which increases cellular ROS (Yu et al., 2009). This activity is best exemplified by 3-AP (aka Triapine®), the only TSC that is currently in clinical trials as an anticancer drug. The mechanism of action of 3-AP has been reportedly due to its inhibition of the iron dependent enzyme, ribonucleotide reductase (RR) (Finch et al., 2000; Finch et al., 1999). The inhibition of this enzyme does not seem to be due to chelation of iron from this enzyme, but rather due to the quenching of the labile tyrosine free radical on the R2 subunit via ROS generated by the TSC-Fe

Molecular Pharmacology Fast Forward. Published on March 20, 2017 as DOI: 10.1124/mol.116.107409
This article has not been copyedited and formatted. The final version may differ from this version.

complexes (Popovic-Bijelic et al., 2011; Shao et al., 2006; Thelander and Graslund, 1983). Consistent with this mechanism, ZMC1-3 all increase ROS similarly to 3-AP.

We have now elucidated another mechanism of action for TSCs as anti-cancer drugs, which is to function as zinc metallochaperones to reactivate mutant p53. The characteristics that define a ZMC have yet to be fully characterized, but at this time zinc K_d, membrane permeability, zinc ionophore activity, and the generation of ROS all seem to play an important role. The exact K_d range that defines a ZMC is unknown; however, our results showing 3-AP with a $K_d > 1\mu M$ combined with our previous observations about control compound A6 ($K_d = 1.1\ \mu M$) provides some clue as to the upper limit.

Given that 3-AP can generate a ROS signal yet cannot function as a ZMC suggests that the ROS signal generated by these four TSCs studied here is related to the iron or perhaps copper binding characterisitics of the drugs (and not zinc). If this is true, then designing chelators that have a greater affinity for zinc and less of an affinity for iron would be optimal for ZMC drug development. Given that the generation of ROS and inhibition of RR (both due to Fe binding) are also mechanisms for toxicity, this would likely result in a compund with more "on target" effects (reactivating mutant p53) and fewer "off target" effects, provided the ROS generation is not reduced so low as to inhibit the ROS-induced transactivation signal required in the ZMC mechanism. That said, it is also possible that there are multiple mechanisms for ROS generation employed by these compounds. Indeed, in addition to the known Fe-dependent mechanism of 3-AP, a recent study by Richardson group indicates that some TSCs induce lysosomal ROS via copper-dependent fenton chemistry (Stefani et al., 2015), and we have not ruled out Zn^{2+}-displacement of redox active metals or other mechnisms arising out of interavtions

Molecular Pharmacology Fast Forward. Published on March 20, 2017 as DOI: 10.1124/mol.116.107409
This article has not been copyedited and formatted. The final version may differ from this version.

with the cellular milieu. If there are multiple ROS generation mechnisms in our ZMCs, the medicinal chemistry may not be so straight-forward.

We have shown that a non-TSC zinc chelator (nitriloacetic acid) can function as a zinc metallochaperone, at least at very high concentration (Yu et al., 2014). While this indicates that the chemical space of metal ion chelators that can function as ZMCs could be potentially large, this work indicates that the TSC class is a useful starting point to explore for undefined ZMCs. This work also leads to the conclusion that not all TSCs are ZMCs. Understanding how to chemically modulate iron and zinc binding seems to be important for this purpose, and ZMC1 and 3-AP with their vastly different zinc binding characteristics can serve as useful tools to understand this.

Molecular Pharmacology Fast Forward. Published on March 20, 2017 as DOI: 10.1124/mol.116.107409
This article has not been copyedited and formatted. The final version may differ from this version.

AUTHORSHIP CONTRIBUTIONS:

Participated in research design: Yu, Blanden, Kimball, Loh, Carpizo

Conducted experiments: Yu, Blanden, Tsang, Zaman, Liu, Gilleran, Bencivenga

Contributed to reagents or analytic tools: Yu, Blanden, Tsang, Zaman, Gilleran, Bencivenga

Performed data analysis: Yu, Blanden, Tsang, Zaman, Loh, Carpizo

Wrote or contributed to the writing of the manuscript: Yu, Blanden, Kimball, Loh, Carpizo

Molecular Pharmacology Fast Forward. Published on March 20, 2017 as DOI: 10.1124/mol.116.107409
This article has not been copyedited and formatted. The final version may differ from this version.

REFERENCES

Beraldo H and Gambino D (2004) The wide pharmacological versatility of semicarbazones, thiosemicarba-zones and their metal complexes. *Mini Rev Med Chem* **4**(1): 31-39.

Bieging KT, Mello SS and Attardi LD (2014) Unravelling mechanisms of p53-mediated tumour suppression. *Nature reviews Cancer* **14**(5): 359-370.

Blanden AR, Yu X, Loh SN, Levine AJ and Carpizo DR (2015a) Reactivating mutant p53 using small molecules as zinc metallochaperones: awakening a sleeping giant in cancer. *Drug Discov Today* **20**(11): 1391-1397.

Blanden AR, Yu X, Wolfe AJ, Gilleran JA, Augeri DJ, O'Dell RS, Olson EC, Kimball SD, Emge TJ, Movileanu L, Carpizo DR and Loh SN (2015b) Synthetic Metallochaperone ZMC1 Rescues Mutant p53 Conformation by Transporting Zinc into Cells as an Ionophore. *Molecular pharmacology* **87**(5): 825-831.

Bozym RA, Thompson RB, Stoddard AK and Fierke CA (2006) Measuring picomolar intracellular exchangeable zinc in PC-12 cells using a ratiometric fluorescence biosensor. *ACS chemical biology* **1**(2): 103-111.

Butler JS and Loh SN (2003) Structure, function, and aggregation of the zinc-free form of the p53 DNA binding domain. *Biochemistry* **42**(8): 2396-2403.

Butler JS and Loh SN (2007) Zn(2+)-dependent misfolding of the p53 DNA binding domain. *Biochemistry* **46**(10): 2630-2639.

Finch RA, Liu M, Grill SP, Rose WC, Loomis R, Vasquez KM, Cheng Y and Sartorelli AC (2000) Triapine (3-aminopyridine-2-carboxaldehyde- thiosemicarbazone): A

potent inhibitor of ribonucleotide reductase activity with broad spectrum antitumor activity. *Biochem Pharmacol* **59**(8): 983-991.

Finch RA, Liu MC, Cory AH, Cory JG and Sartorelli AC (1999) Triapine (3-aminopyridine-2-carboxaldehyde thiosemicarbazone; 3-AP): an inhibitor of ribonucleotide reductase with antineoplastic activity. *Adv Enzyme Regul* **39**: 3-12.

Franken NA, Rodermond HM, Stap J, Haveman J and van Bree C (2006) Clonogenic assay of cells in vitro. *Nat Protoc* **1**(5): 2315-2319.

Freed-Pastor WA and Prives C (2012) Mutant p53: one name, many proteins. *Genes & development* **26**(12): 1268-1286.

Hainaut P and Milner J (1993) A structural role for metal ions in the "wild-type" conformation of the tumor suppressor protein p53. *Cancer Res* **53**(8): 1739-1742.

Haupt Y, Maya R, Kazaz A and Oren M (1997) Mdm2 promotes the rapid degradation of p53. *Nature* **387**(6630): 296-299.

Kunos CA, Radivoyevitch T, Waggoner S, Debernardo R, Zanotti K, Resnick K, Fusco N, Adams R, Redline R, Faulhaber P and Dowlati A (2013) Radiochemotherapy plus 3-aminopyridine-2-carboxaldehyde thiosemicarbazone (3-AP, NSC #663249) in advanced-stage cervical and vaginal cancers. *Gynecol Oncol* **130**(1): 75-80.

Levine AJ and Oren M (2009) The first 30 years of p53: growing ever more complex. *Nature reviews Cancer* **9**(10): 749-758.

Lokshin M, Li Y, Gaiddon C and Prives C (2007) p53 and p73 display common and distinct requirements for sequence specific binding to DNA. *Nucleic acids research* **35**(1): 340-352.

Ma B, Goh BC, Tan EH, Lam KC, Soo R, Leong SS, Wang LZ, Mo F, Chan AT, Zee B and Mok T (2008) A multicenter phase II trial of 3-aminopyridine-2-carboxaldehyde thiosemicarbazone (3-AP, Triapine) and gemcitabine in advanced non-small-cell lung cancer with pharmacokinetic evaluation using peripheral blood mononuclear cells. *Investigational new drugs* **26**(2): 169-173.

Meplan C, Richard MJ and Hainaut P (2000) Metalloregulation of the tumor suppressor protein p53: zinc mediates the renaturation of p53 after exposure to metal chelators in vitro and in intact cells. *Oncogene* **19**(46): 5227-5236.

Murren J, Modiano M, Clairmont C, Lambert P, Savaraj N, Doyle T and Sznol M (2003) Phase I and pharmacokinetic study of triapine, a potent ribonucleotide reductase inhibitor, administered daily for five days in patients with advanced solid tumors. *Clinical cancer research : an official journal of the American Association for Cancer Research* **9**(11): 4092-4100.

Popovic-Bijelic A, Kowol CR, Lind ME, Luo J, Himo F, Enyedy EA, Arion VB and Graslund A (2011) Ribonucleotide reductase inhibition by metal complexes of Triapine (3-aminopyridine-2-carboxaldehyde thiosemicarbazone): a combined experimental and theoretical study. *Journal of inorganic biochemistry* **105**(11): 1422-1431.

Richardson DR, Sharpe PC, Lovejoy DB, Senaratne D, Kalinowski DS, Islam M and Bernhardt PV (2006) Dipyridyl thiosemicarbazone chelators with potent and selective antitumor activity form iron complexes with redox activity. *Journal of medicinal chemistry* **49**(22): 6510-6521.

Shao J, Zhou B, Di Bilio AJ, Zhu L, Wang T, Qi C, Shih J and Yen Y (2006) A Ferrous-Triapine complex mediates formation of reactive oxygen species that inactivate human ribonucleotide reductase. *Mol Cancer Ther* **5**(3): 586-592.

Stefani C, Al-Eisawi Z, Jansson PJ, Kalinowski DS and Richardson DR (2015) Identification of differential anti-neoplastic activity of copper bis(thiosemicarbazones) that is mediated by intracellular reactive oxygen species generation and lysosomal membrane permeabilization. *Journal of inorganic biochemistry* **152**: 20-37.

Thelander L and Graslund A (1983) Mechanism of inhibition of mammalian ribonucleotide reductase by the iron chelate of 1-formylisoquinoline thiosemicarbazone. Destruction of the tyrosine free radical of the enzyme in an oxygen-requiring reaction. *The Journal of biological chemistry* **258**(7): 4063-4066.

Ventura A, Kirsch DG, McLaughlin ME, Tuveson DA, Grimm J, Lintault L, Newman J, Reczek EE, Weissleder R and Jacks T (2007) Restoration of p53 function leads to tumour regression in vivo. *Nature* **445**(7128): 661-665.

Xue W, Zender L, Miething C, Dickins RA, Hernando E, Krizhanovsky V, Cordon-Cardo C and Lowe SW (2007) Senescence and tumour clearance is triggered by p53 restoration in murine liver carcinomas. *Nature* **445**(7128): 656-660.

Yu X, Blanden AR, Narayanan S, Jayakumar L, Lubin D, Augeri D, Kimball SD, Loh SN and Carpizo DR (2014) Small molecule restoration of wildtype structure and function of mutant p53 using a novel zinc-metallochaperone based mechanism. *Oncotarget* **5**(19): 8879-8892.

Yu X, Vazquez A, Levine AJ and Carpizo DR (2012a) Allele-specific p53 mutant reactivation. *Cancer cell* **21**(5): 614-625.

Yu Y, Gutierrez E, Kovacevic Z, Saletta F, Obeidy P, Suryo Rahmanto Y and Richardson DR (2012b) Iron chelators for the treatment of cancer. *Curr Med Chem* **19**(17): 2689-2702.

Yu Y, Kalinowski DS, Kovacevic Z, Siafakas AR, Jansson PJ, Stefani C, Lovejoy DB, Sharpe PC, Bernhardt PV and Richardson DR (2009) Thiosemicarbazones from the old to new: iron chelators that are more than just ribonucleotide reductase inhibitors. *Journal of medicinal chemistry* **52**(17): 5271-5294.

Zeidner JF, Karp JE, Blackford AL, Smith BD, Gojo I, Gore SD, Levis MJ, Carraway HE, Greer JM, Ivy SP, Pratz KW and McDevitt MA (2014) A phase II trial of sequential ribonucleotide reductase inhibition in aggressive myeloproliferative neoplasms. *Haematologica* **99**(4): 672-678.

Molecular Pharmacology Fast Forward. Published on March 20, 2017 as DOI: 10.1124/mol.116.107409
This article has not been copyedited and formatted. The final version may differ from this version.

FOOTNOTES

This work was supported by the National Institute of Health [R01 CA200800, K08CA172676], Sidney Kimmel Foundation for Cancer, and the Breast Cancer Research Foundation, and the National Institute of Health [F30GM113299].

XY and AB contributed equally to this work.

Reprint requests to: Darren R. Carpizo, Rutgers Cancer Institute of New Jersey, 195 Little Albany Street, New Brunswick, NJ 08903. (carpizdr@cinj.rutgers.edu)

Molecular Pharmacology Fast Forward. Published on March 20, 2017 as DOI: 10.1124/mol.116.107409
This article has not been copyedited and formatted. The final version may differ from this version.

LEGENDS FOR FIGURES

Figure 1. *In vitro* evaluation of TSCs as ZMCs. **(A)** Scheme of the four thiosemicarbazones, ZMC1, ZMC2, ZMC3, and 3-AP. **(B)** Competition assay between TSCs and RZ-3. Apparent K_ds were calculated according to Eqn. 1. K_d = 27.4 ± 16.2 (ZMC2), 81.0 ± 34.2 (ZMC3), and >1 μM (3-AP). [RZ-3] = 100 nM, [$ZnCl_2$] = 50 nM. Error bars ± SD (n ≥ 3). **(C)** DBD remetallation assay. R175H and WT DBD's (~20 μM) were apoized and then incubated with a mixture of 180 μM TSC and 60 μM $ZnCl_2$. DBD Zn^{2+}-content was then measured by PAR assay. Error bars ± SD (n ≥ 3). p-values from one way ANOVA with Hilm-Sidak method for multiple comparisons. All three compounds can release metal back to apoized DBD. *p<0.05, **p<0.01, ***p<0.001. **(D)** Fluorescence spectra of proteins remetallated in (C). Gray dotted lines show basis spectra of WT DBD either in buffer alone (native), with 8 M urea (unfolded), or with 10 μM $ZnCl_2$ (misfolded). [DBD] = 0.5 μM. Proteins remetallated with ZMC2 and ZMC3 are mostly native, and with 3-AP are mostly misfolded. **(E-G)** Zn^{2+}-arrested-refolding assays for ZMC2 (E), ZMC3 (F) and 3-AP (G). R175H DBD was unfolded in 5 M urea, then diluted into buffer to the final concentrations of 0.5 μM DBD, 0.1 M urea, and 2.5 μM $ZnCl_2$. Treatments were added at time = 0. Disappearance of the misfolded fluorescence peak was monitored at the isosbestic point between the TSC and TSC-Zn^{2+} complex. Traces shown were corrected empirically for inner filter effect. Gray boxes represent the arrested phase of the experiment. ZMC2 and ZMC3 are able to rescue the folding of R175H DBD, but 3-AP is not. **(H)** Electrophoretic mobility shift assay (EMSA) using R175H DNA binding domain (DBD). apoDBD was incubated with with $ZnCl_2$ (10 μM) and either ZMC1, ZMC2, ZMC3, A6, or 3-AP (20 μM) in TB(noE) buffer

Molecular Pharmacology Fast Forward. Published on March 20, 2017 as DOI: 10.1124/mol.116.107409
This article has not been copyedited and formatted. The final version may differ from this version.

running on 6% native PAGE. Lane 3-7 contained the combination of drug (20 μM) and $ZnCl_2$ (10 μM). Only the ZMC1, ZMC2 and ZMC3 restored site-specific DNA binding to the R175H DBD (Lane 3-5). A6 is used as a negative control. **(I-K)** Zn^{2+}-import kinetics and liposome leakage assay measured by DOPC-encapsulated RZ-3 (red) and CF (green) fluorescence, respectively for ZMC2 (H), ZMC3 (I) and 3-AP (J). Treatments were added at the arrows. RZ-3 was encapsulated at 10 μM and CF at 100 mM. Concentrations shown are: 10 μM $ZnCl_2$, 1 μM TSC, 1 % TritonX-100, and 100 μM EDTA. ZMC2 and ZMC3 have Zn^{2+} ionophore activity, but 3-AP does not. None of the treatments disrupted the liposomes non-specifically. Data represented an average ± SD of 3 experiments performed in triplicate (B-C) and representative data are shown from 3 experiments (D-K).

Figure 2. Thiosemicarbazones with cell growth inhibition activity in cell lines expressing mutant p53. **(A)** Measurement of the sensitivity of the compounds in the cell lines expressing mutant p53. Cell growth inhibition assays was performed in the human tumor cell lines with hotspot p53 mutations by MTS assay. Briefly, cells were treated with eight serial dilutions of the compounds (0.0001 μM to 10 μM) for 3 days. Data represented an average ± SD performed in triplicate, repeated in 3 experiments. **(B)** Cell growth inhibition activity of ZMCs depending on mutant p53. Cell growth inhibition assay was performed in human ovarian cancer cell line TOV112D (p53R175H) by CellTiter-Glo. Data represented an average ± SD performed in triplicate, repeated in 2 experiments. Insert: western blot showed siRNA knockdown to *TP53*. β-actin was used as a loading control. **(C)** Colony formation assay in TOV112D cells. A representative

Molecular Pharmacology Fast Forward. Published on March 20, 2017 as DOI: 10.1124/mol.116.107409
This article has not been copyedited and formatted. The final version may differ from this version.

experiment from triplicates from the three independent experiments is shown. **(D)** A percentage of colonies was obtained for each respective treatment compared with that of DMSO treatment. Data are presented as mean ± SE. *, $P < 0.05$. **, $P < 0.01$.

Figure 3. A "WT-like" conformational change in the p53-175 mutant protein induced by ZMCs. Two $p53^{R175H}$ cell lines TOV112D and SKBR3 cells were treated with ZMC1, ZMC2, ZMC3, and 3-AP (1 μM for 6 hours) and immunofluorescent staining was performed using p53 conformation specific antibodies (PAB1620 for WT conformation and PAB240 for mutant conformation). The scale bar = 100 μm. Representative data are shown from 3 experiments.

Figure 4. Restoration of site-specific p53-175 mutant protein transactivational function by ZMC1, ZMC2 and ZMC3, but not 3-AP. **(A)** TOV112D and SKOV3 cells were treated with ZMC1, ZMC2, ZMC3, or 3-AP, and the gene expression of *p21* and *PUMA* was analyzed by quantitative RT-PCR. The RNA was extracted from the cells using Qiagen RNeasy kit and the gene expression level was measured by quantitative RT-PCR using TaqMan gene expression assays. β-actin was used as the internal control. Data represented an average ± SD performed in triplicate, repeated in 3 experiments. *$p<0.05$, **$p<0.01$, ***$p<0.001$. **(B)** The expression of p21 in TOV112D and SKBR3 cells that were treated with ZMC1, ZMC2, ZMC3, and 3-AP were analyzed by western blot with p21 antibody. β-actin is used as a loading control. Representative data are shown from 3 experiments.

Molecular Pharmacology Fast Forward. Published on March 20, 2017 as DOI: 10.1124/mol.116.107409
This article has not been copyedited and formatted. The final version may differ from this version.

Figure 5. ZMC1 induces ROS levels in cells as detected by 8-oxy-dGUO staining. **(A)** Cells were treated with ZMC1, ZMC2, ZMC3, or 3-AP and stained with 8-oxy-dG antibody. The scale bar represented a size of 100 μm. Representative data are shown from 3 experiments. **(B)** Quantification of staining in TOV112D cells. Representative data are shown from 3 experiments. ***$p<0.001$.

Molecular Pharmacology Fast Forward. Published on March 20, 2017 as DOI: 10.1124/mol.116.107409
This article has not been copyedited and formatted. The final version may differ from this version.

TABLE 1 Cellular sensitivity (EC_{50}) to the four thiosemicarbozone compounds of results shown in Fig. 2A

	ZMC1	ZMC2	ZMC3	3-AP
TOV112D (p53R175H)	0.087 μM	0.087 μM	3.373 μM	1.644 μM
SKBR3 (p53R175H)	0.009 μM	0.009 μM	2.061 μM	>10 μM
HOP92 (p53R175L)	0.291 μM	0.168 μM	1.807 μM	4.246 μM
H1299 (p53 null)	>2 μM	>2 μM	>10 μM	9.661 μM
H460 (p53 wt)	>2 μM	>2 μM	>10 μM	>10 μM

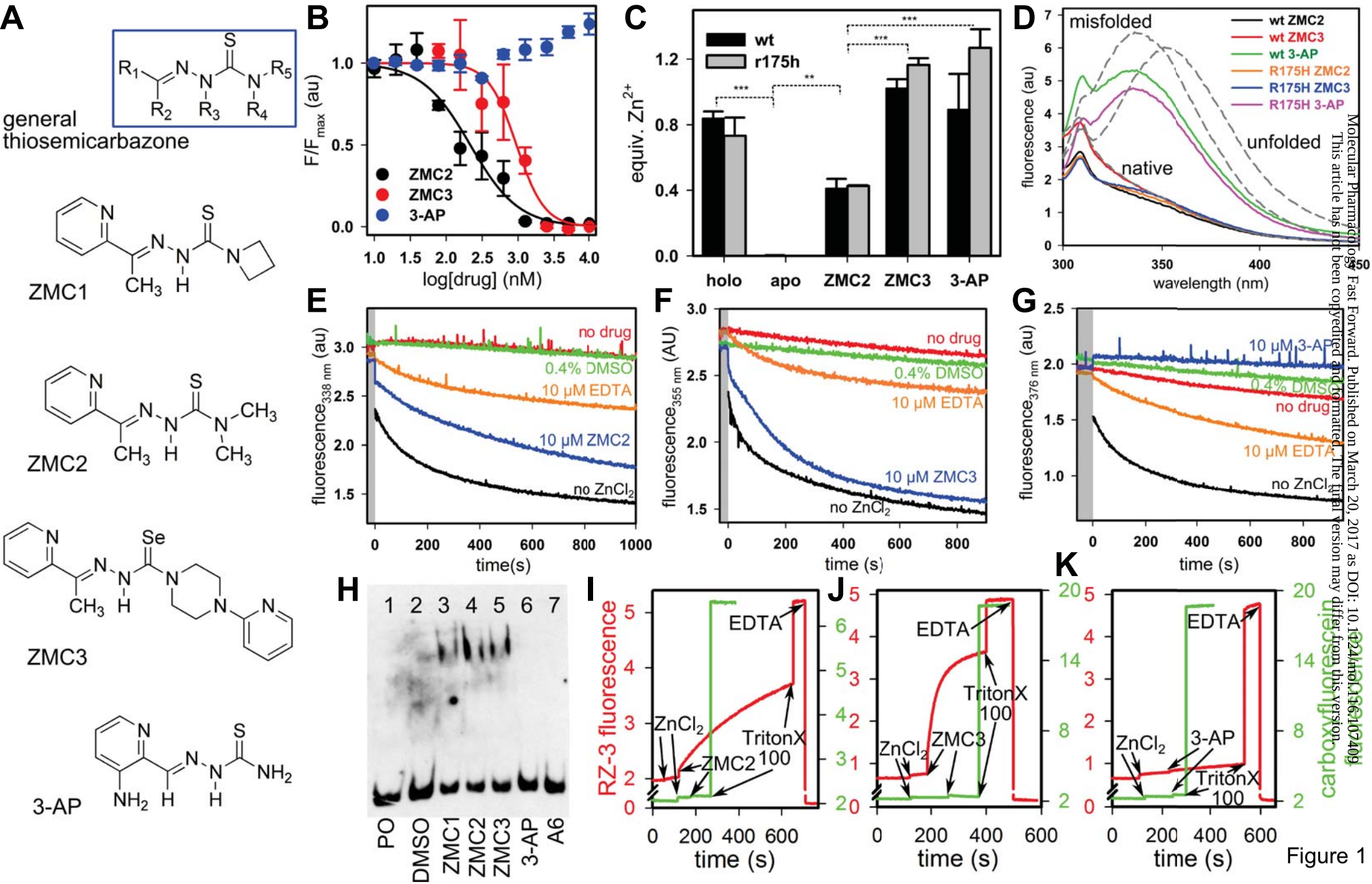

Figure 1

Molecular Pharmacology Fast Forward. Published on March 20, 2017 as DOI: 10.1124/mol.116.107409
This article has not been copyedited and formatted. The final version may differ from this version.

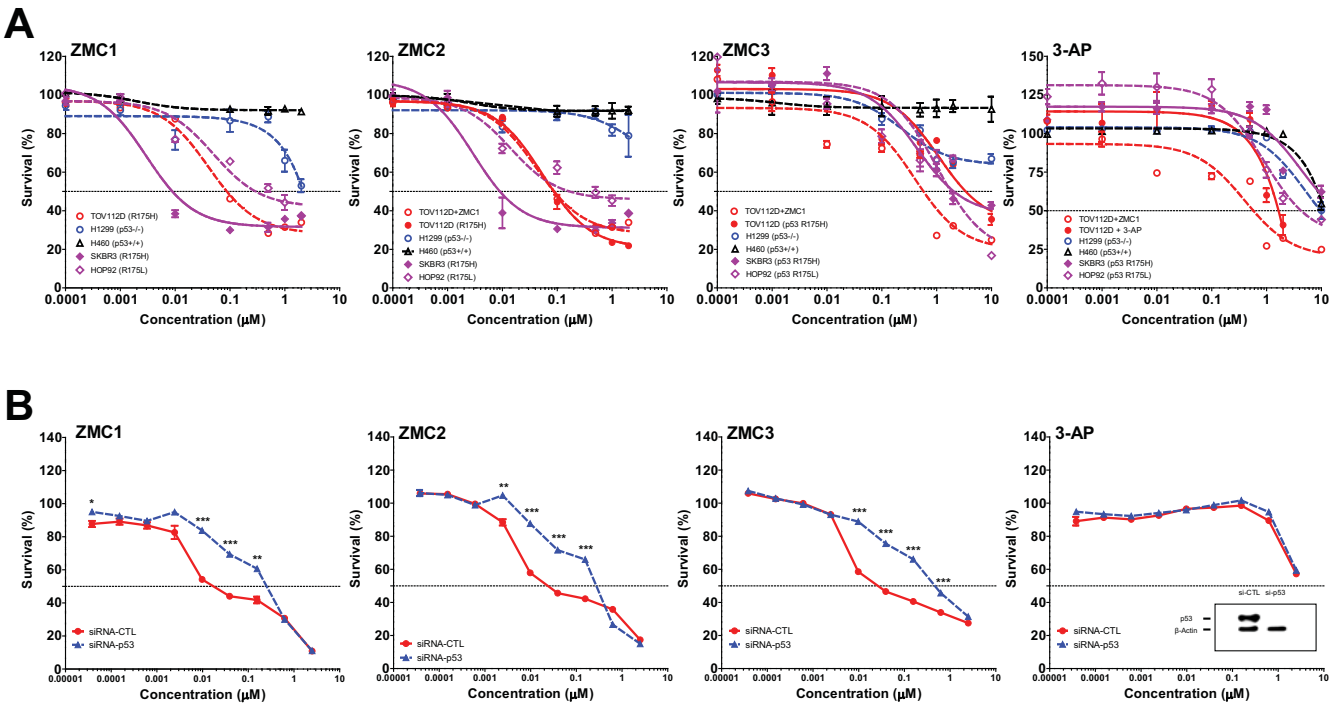

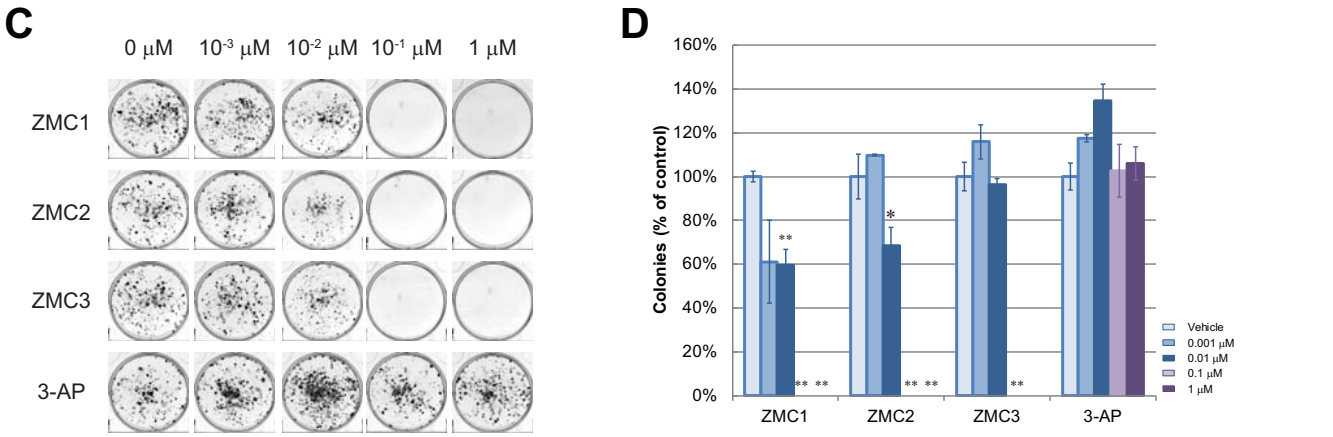

Figure 2

Molecular Pharmacology Fast Forward. Published on March 20, 2017 as DOI: 10.1124/mol.116.107409
This article has not been copyedited and formatted. The final version may differ from this version.

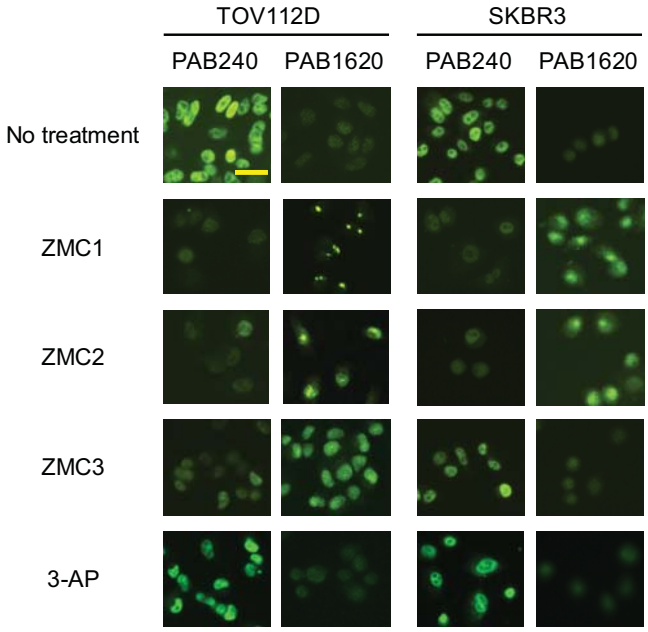

Figure 3

Molecular Pharmacology Fast Forward. Published on March 20, 2017 as DOI: 10.1124/mol.116.107409
This article has not been copyedited and formatted. The final version may differ from this version.

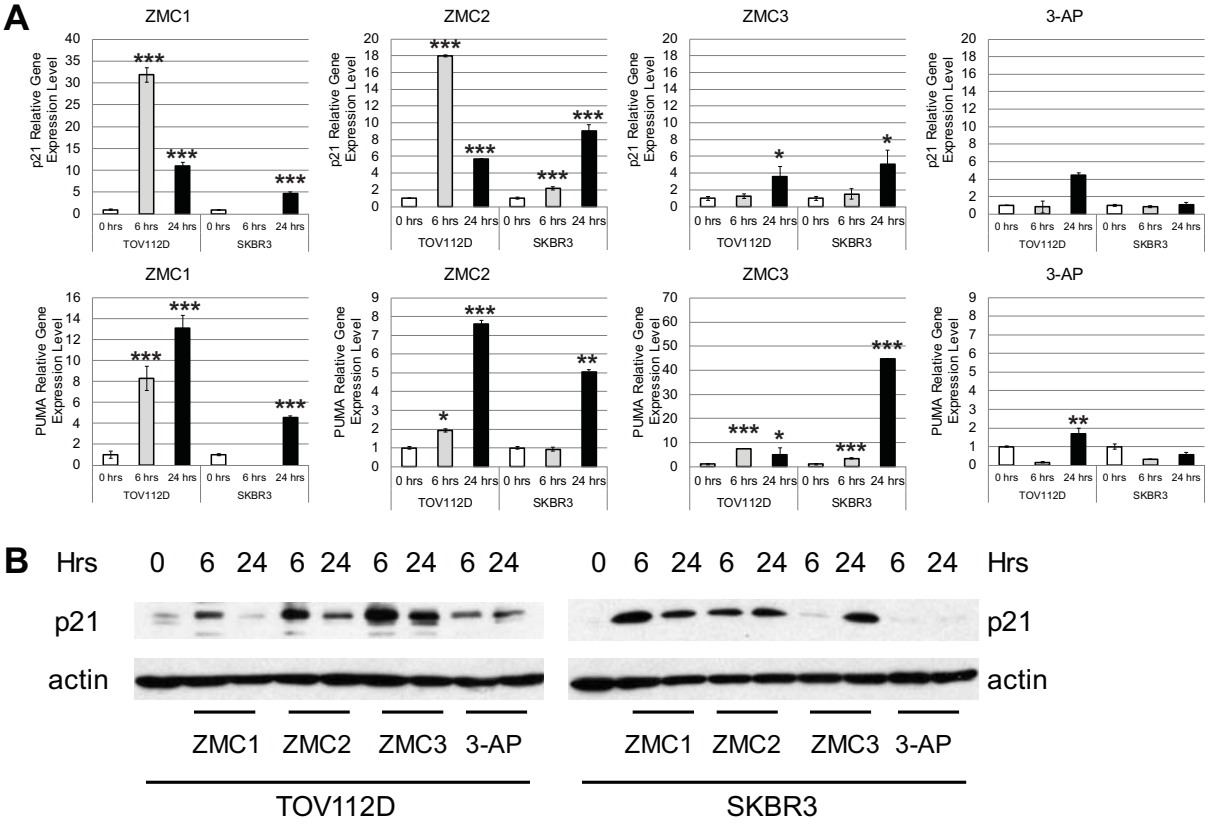

Figure 4

Molecular Pharmacology Fast Forward. Published on March 20, 2017 as DOI: 10.1124/mol.116.107409
This article has not been copyedited and formatted. The final version may differ from this version.

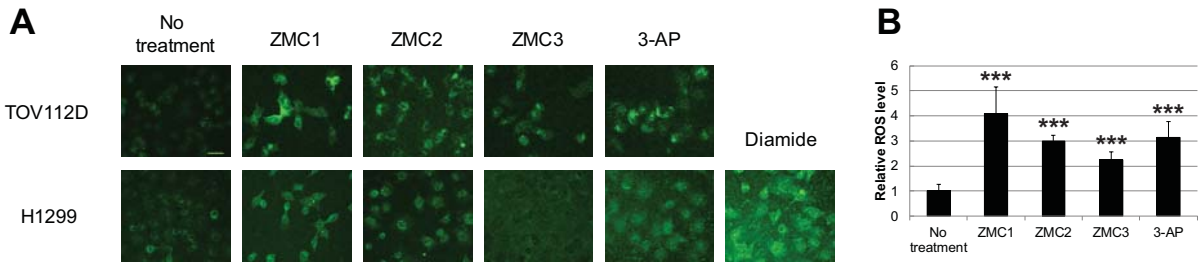

Figure 5